ChemComm

COMMUNICATION

View Article Online
View Journal | View Issue

Cite this: *Chem. Commun.*, 2015, **51**, 5735

Received 24th January 2015,
Accepted 18th February 2015

DOI: 10.1039/c5cc00686d

www.rsc.org/chemcomm

Photocatalytic CO_2 reduction by a mixed metal (Zr/Ti), mixed ligand metal–organic framework under visible light irradiation†

Yeob Lee,[a] Sangjun Kim,[b] Jeung Ku Kang*[bc] and Seth M. Cohen*[a]

Postsynthetic exchange (PSE) of Ti(IV) into a Zr(IV)-based MOF enabled photocatalytic CO_2 reduction to HCOOH under visible light irradiation with the aid of BNAH and TEOA. Use of a mixed-ligand strategy enhanced the photocatalytic activity of the MOF by introducing new energy levels in the band structure of the MOF.

Carbon dioxide (CO_2) produced by energy generation based on fossil fuels contributes to global warming and consequently negative effects on the environment.[1–3] Direct conversion of CO_2 into useful chemicals is regarded as a promising technology for addressing the CO_2 problem.[4] Inspired by nature, systems that can photocatalytically generate hydrocarbon fuels from CO_2 have gathered substantial interest. Homogeneous systems based on transition metal centers with photosensitizers can show high efficiencies, but they are generally not reusable.[5] On the other hand, heterogeneous photocatalysts based on semiconductors are robust, but suffer from low efficiencies because most of these systems only absorb UV light, which represents only ~4% of the solar energy spectrum.[6] Developing new photocatalysts that can harvest more of the solar spectrum, while retaining high stability and efficiency, would be an important advancement for CO_2 utilization.

Metal–organic frameworks (MOFs) are crystalline hybrid materials for CO_2 conversion with high specific surface area, because they can be tuned by design.[7–10] The use of MOFs in photocatalysis of CO_2 has been investigated.[11,12] Fu *et al.* found that Ti-based NH_2-MIL-125(Ti) could mediate the conversion of CO_2 to $HCOO^-$ in the presence of triethanolamine (TEOA). In addition, they found that visible light sensitivity could be introduced by incorporating 2-aminobenzene-1,4-dicarboxylic acid (NH_2-bdc).[11] Another work also used NH_2-MIL-125(Ti) to produce H_2 from a TEOA–H_2O solution under visible light irradiation.[13]

Now a well studied, robust, and highly porous MOF, UiO-66 (UiO = University of Oslo) constructed from Zr secondary-building units (SBUs) and benzene-1,4-dicarboxylic acid (H_2bdc),[14–18] cannot catalyze the reduction of CO_2 to $HCOO^-$ or the reduction of H_2O to H_2. The Zr_6 SBUs ($Zr_6O_4(OH)_4$) cannot accept electrons from the bdc linker under light irradiation (unlike the aforementioned Ti_8 SBUs ($Ti_8O_8(OH)_4$)) because the redox potential energy level of the Zr_6 SBUs in UiO-66 lies above the LUMO of the bdc ligands.[12,13,19] Consequently, it was hypothesized that embedding Ti ions into the Zr_6 SBUs of UiO-66 might introduce catalytic activity to UiO-66 by lowering the redox potential energy of the Zr_6 cluster.

Herein, we report a mixed-ligand, mixed-metal UiO-66-derivative ($Zr_{4.3}Ti_{1.7}O_4(OH)_4(C_8H_7O_4N)_{5.17}(C_8H_8O_4N_2)_{0.83}$, **1(Zr/Ti)**) obtained by postsynthetic exchange (PSE)[20–26] as an effective photocatalyst for CO_2 reduction under visible light irradiation. The Ti(IV) ions make the SBUs capable of accepting electrons generated *via* light absorption by the organic linkers. Introducing a small amount of 2,5-diaminobenzene-1,4-dicarboxylic acid ($(NH_2)_2$-bdc) as a co-ligand provided new energy levels in the band structure of the MOF and introduced broader light absorption coverage for the MOF (Scheme 1).

Solvothermal synthesis of **1(Zr)** produced nanocrystals with excellent crystallinity (Fig. 1) and a narrow size distribution (Fig. S1, ESI†). The crystal growth of **1(Zr)** gave particles with an edge length of ~70 nm, which is smaller than that obtained for UiO-66(Zr)-NH_2 at around ~200 nm. **1(Zr)** absorbed visible light as shown by two broad absorption bands in the UV-vis spectrum, while UiO-66(Zr)-NH_2 absorbs only a small portion of blue light beyond the UV spectrum (Fig. S2, ESI†). The ratio between NH_2-bdc and $(NH_2)_2$-bdc was calculated by dissolving the MOF under alkaline conditions and measuring the ^{1}H NMR spectrum in solution (see ESI†). **1(Zr)** contained ~14% $(NH_2)_2$-bdc and 86% NH_2-bdc, which is slightly different from the

[a] *Department of Chemistry and Biochemistry, University of California, San Diego, La Jolla, California 92093, USA. E-mail: scohen@ucsd.edu*
[b] *Department of Materials Science and Engineering, Korea Advanced Institute of Science and Technology (KAIST), Daejeon, 305-701, Republic of Korea. E-mail: jeung@kaist.ac.kr*
[c] *Graduate School of EEWS, Korea Advanced Institute of Science and Technology (KAIST), Daejeon, 305-701, Republic of Korea*

† Electronic supplementary information (ESI) available: Experimental, details of results. See DOI: 10.1039/c5cc00686d

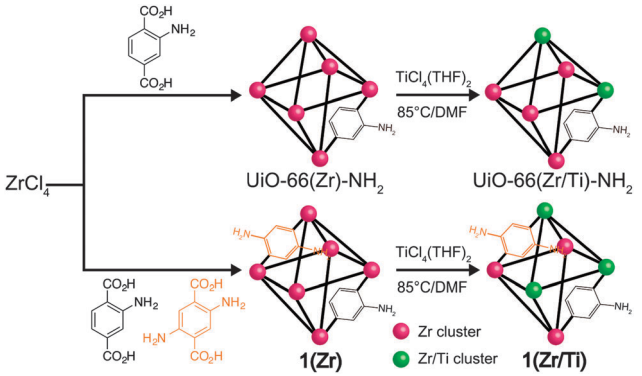

Scheme 1 Synthesis of mixed-ligand MOF **1(Zr)** *via* PSE to obtain mixed-metal MOFs **1(Zr/Ti)**, UiO-66(Zr/Ti)-NH_2.

ligand ratio used in synthesis of the MOF (this may be due to the lower solubility of $(NH_2)_2$-bdc in *N*,*N*-dimethylformamide (DMF)). Afterwards, these Zr-based MOFs were exposed to DMF solutions of $TiCl_4(THF)_2$ for 5 days at 85 °C in order to achieve PSE with Ti(IV).

After PSE, the crystallinity, morphology, and light absorption of the UiO-66 materials were maintained, indicating that PSE did not alter the gross physical properties of the MOFs. Introduction of Ti(IV) into the MOF was confirmed by both energy-dispersive X-ray spectroscopy (EDS) and inductively-coupled plasma mass spectrometry (ICP-MS) measurements. The ratios for Zr/Ti were 2.52 for **1(Zr/Ti)** and 3.03 for UiO-66(Zr/Ti)-NH_2 as determined by ICP-MS (Table S1, ESI†). The ICP-MS data support our argument that Ti(IV) was substituted for Zr(IV) in MOF SBUs. The weight percentage of both elements in **1(Zr/Ti)** was determined to be 23.2 wt% for Zr and 4.8 wt% for Ti. If Ti was simply loaded into **1(Zr)** with no change in the SBUs, then these values should be 29.2 wt% for Zr and 6.1 wt% for Ti (Table S2, ESI†). Furthermore, the surface area of **1(Zr)** was essentially unchanged after PSE (from 937 ± 7 $m^2\ g^{-1}$ to 1004 ± 9 $m^2\ g^{-1}$), indicating that the added Ti is not blocking the pores of the MOF. These suggest that, on average, the Zr_6 SBUs were converted by PSE to $\sim Zr_{4.3}Ti_{1.7}$ for **1(Zr/Ti)** and $\sim Zr_{4.5}Ti_{1.5}$ for UiO-66(Zr/Ti)-NH_2.

Both MOFs were tested for photocatalytic CO_2 reduction under visible light irradiation. The reaction was conducted in 5 mL of a mixed solution of 4 : 1 (v/v) acetonitrile (MeCN)–triethanolamine (TEOA, as a sacrificial base), and 0.1 M 1-benzyl-1,4-dihydronicotinamide (BNAH, as a sacrificial reductant).[27–29] The suspension, which contained 5 mg of MOF, was purged with 1 bar of CO_2 gas for 30 min followed by light irradiation by a 300 W Xe lamp. The initial pH value of the 4 : 1 MeCN–TEOA solution was ~11, but dropped to ~9.5 after purging with CO_2 gas. Because of the high pH, the photocatalysis products can be deprotonated; therefore, the reaction mixtures were extracted with ethyl acetate and washed with H_2SO_4 (to remove TEOA and protonated products).[30] The final ethyl acetate solution (1 μL) was analyzed by gas chromatography-mass spectrometry (GC-MS) to identify the products.

The photocatalysis products were analyzed *via* GC-MS, the results of which are shown in Fig. 2. **1(Zr/Ti)** showed similar

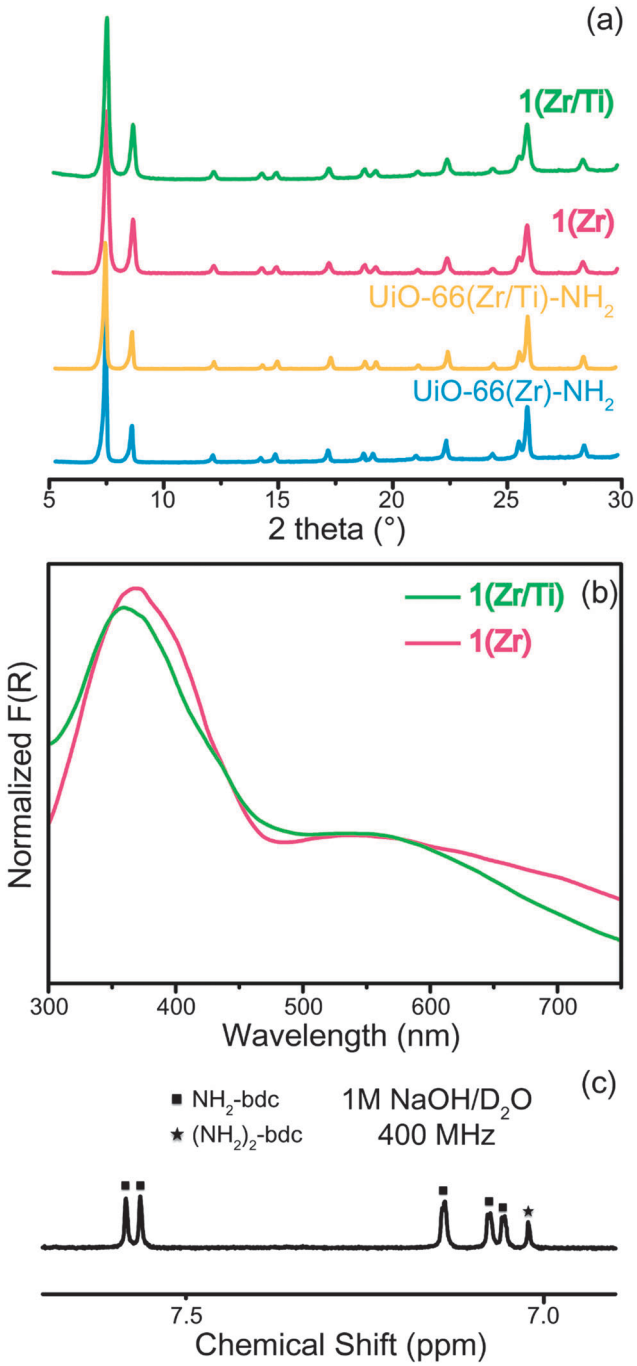

Fig. 1 (a) PXRD patterns of UiO-66(Zr)-NH_2, UiO-66(Zr/Ti)-NH_2, **1(Zr)**, and **1(Zr/Ti)**. (b) Diffuse reflectance UV-visible spectra of **1(Zr)** and **1(Zr/Ti)** (calculated using the Kubelka–Munk function, $F(R)$). (c) ^1H NMR of dissolved **1(Zr)**.

turnover number values over three photocatalytic cycles (6 hours each), indicating that the catalytic ability of the MOF was not degraded during photocatalysis. Turnover numbers were calculated based on the Ti content determined from ICP-MS results. The average turnover number of 6.27 ± 0.23 (31.57 ± 1.64 μmol of HCOOH, from 3 independent samples) indicates that each Ti site transferred about 13 electrons to CO_2 over the course of each catalytic run (Fig. S3, ESI†). UiO-66(Zr/Ti)-NH_2 gave a lower

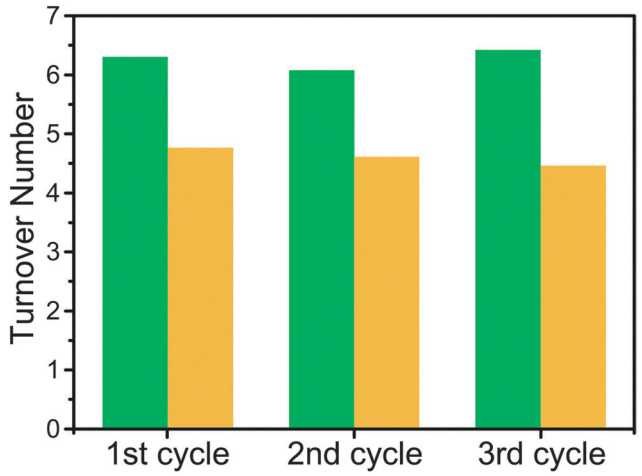

Fig. 2 Turnover numbers of **1(Zr/Ti)** (green) and UiO-66(Zr/Ti)-NH_2 (gold) for photocatalysis of CO_2 to HCOOH over three cycles. Samples were recovered after each cycle and reused under identical reaction conditions.

turnover number (4.66 ± 0.17) when compared to **1(Zr/Ti)** (Fig. 2 and Fig. S4, ESI†). No HCOOH was detected when using the parent **1(Zr)** and UiO-66(Zr)-NH_2 materials, indicating that Ti was essential for photocatalysis.

The MOFs were studied by photoluminescence (PL) spectroscopy to provide evidence for charge transfer in **1(Zr/Ti)**. As shown in Fig. 3a, the emission intensity of **1(Zr)** was remarkably reduced after PSE. This indicates that the recombination rate of photogenerated electron–hole pairs in the organic linkers was decreased suggesting that charges were transferred to the inorganic SBUs. In addition, **1(Zr/Ti)** achieved better charge separation than UiO-66(Zr/Ti)-NH_2 because **1(Zr/Ti)** quenched a greater portion of the photogenerated charges than UiO-66(Zr/Ti)-NH_2 (Fig. S5, ESI†). This indicates that **1(Zr/Ti)** accepts more electrons from the organic linkers to catalyze CO_2 than UiO-66(Zr/Ti)-NH_2, which is supported by the GC-MS results.

The energy band structures of both **1(Zr/Ti)** and UiO-66(Zr/Ti)-NH_2 were investigated using UV light photo-electron spectroscopy (UPS, Fig. S6, ESI†). The UPS results indicate that **1(Zr/Ti)** has two different valence bands, in contrast to UiO-66(Zr/Ti)-NH_2 that has a single valence band. This is consistent with the UV-visible spectra in Fig. 1(b) where **1(Zr/Ti)** showed two absorption bands.

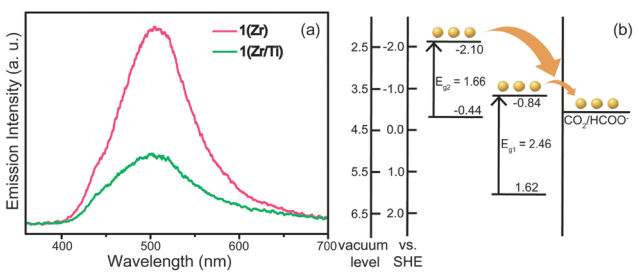

Fig. 3 (a) Photoluminescence spectra of both **1(Zr)** and **1(Zr/Ti)**. (b) Energy band structure of **1(Zr/Ti)** derived from UPS and *F*(*R*) results. Heterogeneous ligands formed two energy levels in MOF, which potentially catalyze CO_2.

The maxima of the two valence bands of **1(Zr/Ti)** were calculated to be 1.62 eV and −0.44 eV (*vs.* SHE) from the UPS spectrum of **1(Zr/Ti)** and bandgap energies for those two levels were determined from UV-vis spectra to be 2.46 eV and 1.66 eV, respectively. These data can be used to produce an energy band diagram of **1(Zr/Ti)** as shown in Fig. 3(b). Two conduction band minima values of −0.84 eV and −2.10 eV (*vs.* SHE) are suitable for electron transfer to CO_2.[31] UiO-66(Zr/Ti)-NH_2 has a single valence band maximum of 1.88 eV and its conduction band minimum was calculated to be −0.79 eV based on the bandgap energy for UiO-66(Zr/Ti)-NH_2 of 2.67 eV (calculated from the UV-vis spectrum, Fig. S7, ESI†). Consequently, **1(Zr/Ti)** is expected to show better photocatalytic efficiency than UiO-66(Zr/Ti)-NH_2 because **1(Zr/Ti)** has two light absorption routes (both suitable for CO_2 reduction) originating from the $(NH_2)_2$-bdc ligand.

In order to prove that HCOOH is produced from photocatalytic reduction of CO_2, the reaction was performed using $^{13}CO_2$ and the products analyzed by ^{13}C NMR. A solution containing CD_3CN, TEOA, BNAH, and $^{13}CO_2$ was subjected to identical photocatalysis conditions (see ESI†). Calibration of the expected product peaks was performed because the alkaline reaction conditions can perturb the chemical shifts of the products (Fig. S8, ESI†).[30] $H^{13}COOH$ was found at 162.73 ppm in a CD_3CN solution and this value was increased to 169.86 ppm due to deprotonation of $H^{13}COOH$ to $H^{13}COO^-$ with added TEOA.

Several products, including $H^{13}COO^-$, $^{13}CO_2$, $H^{13}CO_3^{2-}$, $^{13}CO_3^{2-}$, residual solvent, and other small peaks were found in the ^{13}C NMR spectrum after photocatalysis by both **1(Zr/Ti)** after 13 hours of light irradiation (Fig. 4). $^{13}CO_3^{2-}$ and $H^{13}CO_3^{2-}$ were produced by oxidation of $^{13}CO_2$ under these alkaline conditions.[31,32] Other small peaks come from isotopes of BNAH as these shifts were found in a reference solution of CD_3CN–TEOA–BNAH (Fig. S8, ESI†). These results indicate that the carbon source of photocatalytically produced HCOOH is CO_2 gas, and not other sources (such as MOF ligand decomposition). The ^{13}C NMR spectrum of the product solution from UiO-66(Zr/Ti)-NH_2 showed additional peaks in addition to BNAH and these peaks might represent organic linkers dissociated from the MOF during photocatalysis (Fig. S9, ESI†). No $H^{13}COO^-$ was detected in NMR spectra when using **1(Zr)** and UiO-66(Zr)-NH_2, consistent with the GC-MS results.

Durability is another important issue when considering long-term photocatalysis. The crystallinity, Zr/Ti ratio, and morphology of the UiO-66 materials were examined after three

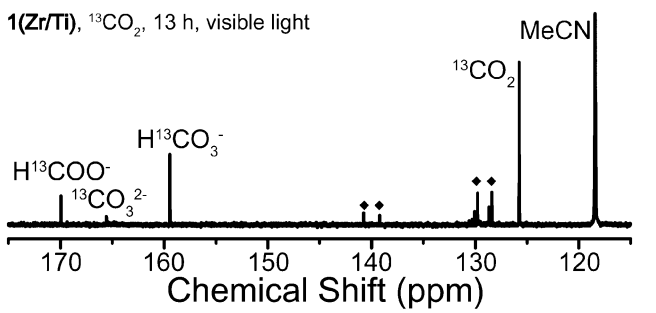

Fig. 4 ^{13}C NMR spectrum of product solution from photocatalysis of $^{13}CO_2$ by **1(Zr/Ti)** for 13 hours under visible light irradiation. ◆ = BNAH.

cycles of photocatalysis. Both **1(Zr/Ti)** and UiO-66(Zr/Ti)-NH_2 maintained the crystallinity and morphology after three cycles of photocatalysis (Fig. S10 and S11, ESI†). However, UiO-66(Zr/Ti)-NH_2 showed broadened PXRD reflections, a roughened surface in SEM image, and greater leaching of Ti (as measured by ICP-MS, Table S1, ESI†), compared to **1(Zr/Ti)**. Overall, **1(Zr/Ti)** was more stable than UiO-66(Zr/Ti)-NH_2 during photocatalysis.

To evaluate our mixed-metal approach, the photocatalytic activity of NH_2-MIL-125(Ti) was also investigated. NH_2-MIL-125(Ti) was synthesized following a reported procedure and its structure confirmed by PXRD (Fig. S12, ESI†).[13] Photocatalysis with NH_2-MIL-125(Ti) under the same reaction conditions described above gave a turnover number of 1.52 after 6 hours. This value is much lower when compared to the MOFs described here. Therefore, it is inferred that the mixed metal SBUs described here are more efficient photocatalysts. This might be, in part, because the Ti_8 SBUs have a redox potential that is too low to provide a sufficient driving force to catalyze CO_2 reduction when compared to the mixed Zr/Ti SBUs described here.

The photocatalytic ability of **1(Zr/Ti)** was also compared to heterogeneous photocatalytic systems based on semiconductors or MOFs in units of turnover frequency (h^{-1}) (Tables S3 and S4, ESI†).[33–38] **1(Zr/Ti)** prepared in this work showed a much higher photocatalytic ability, and also improved visible light sensitivity than non-MOF heterogeneous photocatalysts. In the comparison to MOF-based photocatalysts, only one MOF system we are aware of shows better catalytic ability than **1(Zr/Ti)**, but this system requires Ru for both the catalytic site and an exogenous light sensitizer.[38] In the latter example, the reaction conditions are not identical to those reported here, which makes an absolute comparison of photoreactivity difficult.

In summary, highly efficient and robust MOF photocatalysts for CO_2 reduction to HCOOH under visible light irradiation, without the need for an exogenous light sensitizer, were developed *via* PSE of Ti(IV) into a series of UiO-66 MOFs. UiO-66 materials were tuned to have catalytic activity by lowering the electron accepting levels of the $Zr_{6-x}Ti_x$ ($Zr_{6-x}Ti_xO_4(OH)_4$) SBUs. Introduction of diamine-substituted ligands greatly enhanced the photocatalytic ability by introducing new energy levels for additional light absorption and charge transfer. This study suggests a new approach to develop MOF photocatalysts using a mixed-metal and mixed-linker approach.

The majority of the experiments described, including all of the synthetic work and MOF characterization, was supported by a grant from the Department of Energy, Office of Basic Energy Sciences, Division of Materials Science and Engineering under Award No. DE-FG02-08ER46519 (Y.L., S.M.C.). Additional support for S.K. and J.K.K. was provided by the Korea Center for Artificial Photosynthesis (KCAP) funded by the National Research Foundation of Korea (2009-0093881).

Notes and references

1 H. D. Matthews, N. P. Gillett, P. A. Stott and K. Zickfeld, *Nature*, 2009, **459**, 829–832.
2 S. J. Davis, K. Caldeira and H. D. Matthews, *Science*, 2010, **329**, 1330–1333.
3 N. S. Lewis and D. G. Nocera, *Proc. Natl. Acad. Sci. U. S. A.*, 2006, **103**, 15729–15735.
4 E. V. Kondratenko, G. Mul, J. Baltrusaitis, G. O. Larrazábal and J. Pérez-Ramírez, *Energy Environ. Sci.*, 2013, **6**, 3112–3135.
5 A. J. Morris, G. J. Meyer and E. Fujita, *Acc. Chem. Res.*, 2009, **42**, 1983–1994.
6 Y. Qu and X. Duan, *Chem. Soc. Rev.*, 2013, **42**, 2568–2580.
7 K. Sumida, *et al.*, *Chem. Rev.*, 2012, **112**, 724–781.
8 J. R. Li, J. Sculley and H. C. Zhou, *Chem. Rev.*, 2012, **112**, 869–932.
9 M. Yoon, R. Srirambalaji and K. Kim, *Chem. Rev.*, 2012, **112**, 1196–1231.
10 J. Della Rocca, D. Liu and W. Lin, *Acc. Chem. Res.*, 2011, **44**, 957–968.
11 Y. Fu, *et al.*, *Angew. Chem., Int. Ed.*, 2012, **51**, 3364–3367.
12 S. Wang, W. Yao, J. Lin, Z. Ding and X. Wang, *Angew. Chem., Int. Ed.*, 2014, **53**, 1034–1038.
13 Y. Horiuchi, *et al.*, *J. Phys. Chem. C*, 2012, **116**, 20848–20853.
14 L. Valenzano, *et al.*, *Chem. Mater.*, 2011, **23**, 1700–1718.
15 Q. Yang, *et al.*, *Chem. Commun.*, 2011, **47**, 9603–9605.
16 M. Kim and S. M. Cohen, *CrystEngComm*, 2012, **14**, 4096–4106.
17 M. Servalli, M. Ranocchiari and J. A. Van Bokhoven, *Chem. Commun.*, 2012, **48**, 1904–1906.
18 F. Vermoortele, *et al.*, *J. Am. Chem. Soc.*, 2013, **135**, 11465–11468.
19 W. Liang, R. Babarao and D. M. D'Alessandro, *Inorg. Chem.*, 2013, **52**, 12878–12880.
20 M. Kim, J. F. Cahill, Y. Su, K. A. Prather and S. M. Cohen, *Chem. Sci.*, 2012, **3**, 126–130.
21 O. Karagiaridi, *et al.*, *Chem. Sci.*, 2012, **3**, 3256–3260.
22 M. Kim, J. F. Cahill, H. Fei, K. A. Prather and S. M. Cohen, *J. Am. Chem. Soc.*, 2012, **134**, 18082–18088.
23 S. Takaishi, E. J. DeMarco, M. J. Pellin, O. K. Farha and J. T. Hupp, *Chem. Sci.*, 2013, **4**, 1509–1513.
24 S. Pullen, H. Fei, A. Orthaber, S. M. Cohen and S. Ott, *J. Am. Chem. Soc.*, 2013, **135**, 16997–17003.
25 H. Fei, *et al.*, *J. Am. Chem. Soc.*, 2014, **136**, 4965–4973.
26 H. Fei, S. Pullen, A. Wagner, S. Ott and S. M. Cohen, *Chem. Commun.*, 2015, **51**, 66–69.
27 Y. Tamaki, T. Morimoto, K. Koike and O. Ishitani, *Proc. Natl. Acad. Sci. U. S. A.*, 2012, **109**, 15673–15678.
28 C. Pac, M. Ihama, M. Yasuda, Y. Miyauchi and H. Sakurai, *J. Am. Chem. Soc.*, 1981, **103**, 6495–6497.
29 X. Q. Zhu, *et al.*, *Chem. – Eur. J.*, 2003, **9**, 3937–3945.
30 H. Takeda, H. Koizumi, K. Okamoto and O. Ishitani, *Chem. Commun.*, 2014, **50**, 1491–1493.
31 T. Reda, C. M. Plugge, N. J. Abram and J. Hirst, *Proc. Natl. Acad. Sci. U. S. A.*, 2008, **105**, 10654–10658.
32 S. Moret, P. J. Dyson and G. Laurenczy, *Dalton Trans.*, 2013, **42**, 4353–4356.
33 X.-H. Xia, *et al.*, *Carbon*, 2007, **45**, 717–721.
34 T. Baran, S. Wojtyła, A. Dibenedetto, M. Aresta and W. Macyk, *Appl. Catal., B*, DOI: 10.1016/j.apcatb.2014.09.052.
35 Q. Zhang, C.-F. Lin, Y. H. Jing and C.-T. Chang, *J. Air Waste Manage. Assoc.*, 2014, **64**, 578–585.
36 G. Mele, *et al.*, *Molecules*, 2015, **20**, 396–415.
37 L. Li, *et al.*, *Chem. Sci.*, 2014, **5**, 3808–3813.
38 D. Sun, *et al.*, *Chem. Commun.*, 2015, **51**, 2645–2648.

